Journal of Applied Analysis and Computation
Volume 16, Number 3, June 2026, 1207–1225
Website:http://www.jaac-online.com
DOI:10.11948/20250104

A RUBELLA EPIDEMIC MODEL WITH SEASONALITY

Yandan Zhang[1], Tailei Zhang[1] and Zhimin Li[1,2,†]

Abstract In this paper, we formulate a periodic SVPEAIRS model based on the transmission features of rubella. We define the basic reproduction number $\mathcal{R}_0$ and show that the disease-free equilibrium is globally asymptotically stable when $\mathcal{R}_0 < 1$. The disease is uniformly persistent and there is at least one positive periodic solution when $\mathcal{R}_0 > 1$. Numerically, we find that rubella cases in China fluctuate periodically with seasonal changes. Furthermore, when the vaccination rate significantly drops from 0.3 to 0.15, or the recovery rate decreases from 0.6 to 0.3, the rubella epidemic will show an explosive growth trend. This finding emphasizes the great significance of maintaining a high vaccination coverage rate and improving the efficiency of medical treatment in preventing the large-scale spread of rubella. Finally, we analyze the bifurcation phenomenon of the model.

Keywords Rubella, seasonal patterns, basic reproduction number, threshold dynamics.

MSC(2010) 34A34, 34C60, 92C40, 92D30.

1. Introduction

Rubella is a highly contagious viral infection transmitted through direct contact or respiratory droplets. The average incubation period is 14 days (range: 12–21 days). It primarily affects children aged 1–5 years, with frequent preschool outbreaks. Children typically experience mild symptoms, while adults may develop headaches and arthralgia. Rare complications include thrombocytopenia and encephalitis (encephalitis occurs in approximately 1 in 6,000 cases and can be fatal). Up to 50% of rubella infections may be asymptomatic [19, 20]. Even in clinically asymptomatic pregnant women, the virus can cause transplacental transmission, leading to Congenital Rubella Syndrome (CRS). CRS manifests as severe birth defects, stillbirth, or preterm delivery etc.

Rubella high-incidence areas are predominantly concentrated in regions with low vaccination coverage. These regions include Africa and Southeast Asia. The Philippines experienced a dramatic surge in cases in 2024. A total of 2,264 cases were reported by April 27. This number is over five times higher than the 397 cases reported during the same period in 2023. This highlights the correlation between vaccination rates and disease incidence. Elimination strategies must integrate local epidemiological characteristics. Strategies should also consider historical vaccination coverage. Health system capacity must be factored into planning. Currently, all Member States implement routine two dose vaccination schedules for measles and rubella, typically using combination vaccines such as the measles-mumps-rubella (MMR) vaccine [20]. The goals of the MRI were to achieve at least a 95% reduction in global measles mortality and to eliminate measles and rubella in at least five of the six WHO regions [15].

[†]The corresponding author.
[1]School of Science, Chang'an University, Xi'an 710064, China
[2]Complex Systems Research Center, Shanxi University, Taiyuan 030006, China
Email: ydzhang2001@126.com(Y. Zhang), t.l.zhang@126.com(T. Zhang), zmli@chd.edu.cn(Z. Li)

The public health impacts and transmission patterns of rubella have been extensively studied. Mathematical models have been developed to predict and control outbreaks. For instance, Prawoto et al. proposed a definitive SEIRV model to study the dynamics of vaccine associated rubella infection [13]. Yang, Freitas developed the SEIVR model to eliminate and reduce rubella and CRS using vaccination strategies [21]. Qurashi developed a fractional SEIR model of rubella epidemics [14]. Tilahun et al. constructed the deterministic and stochastic mathematical model SVPIR, taking into account the vertical transmission and environmental factors, in order to understand the transmission dynamics of rubella. [16]. Adewale et al. researched and developed a mathematical model SVPITR to simulate the transmission pattern of rubella [1]. Their modelling studies show that reducing exposure and vertical transmission rates, and increasing recovery rates, vaccination rates, and maternal immunization are critical to mitigating the impact of rubella on populations.

Rubella incidence exhibits distinct seasonality. This seasonal pattern is associated with climate conditions, population density, and viral transmission characteristics. In China, rubella epidemics follow clear spatiotemporal patterns. The annual incidence peaks consistently occur from March to June. This seasonal regularity provides critical evidence for formulating prevention strategies and immunization policies [11]. Many researchers have conducted in-depth research on periodic issues. Han et al. addressed the stability of periodic solutions of piecewise smooth periodic dierential equations [6]. Carvalho et al. analyzed a periodically-forced dynamical system inspired by the SIR model with impulsive vaccination [4]. Ochieng investigated an improved susceptibility-exposure-infection-recovery-susceptibility (SEIRS) compartment mathematical model to assess the impact of awareness-based control measures on the dynamics of malaria transmission, including mosquito interactions and seasonality [12].

According to the ideas of [7, 9, 10, 17], we introduce a time-periodic compartment model. Recognizing that the basic transmission rate is the key parameter influencing seasonality, we introduce a cyclical transmission rate $\beta(t)$ between susceptible and symptomatic individuals. In our model, we differentiate between symptomatic and asymptomatic infected individuals. Given that rubella immunoprophylaxis is the most effective strategy for controlling the rubella epidemic and its associated harms, we also include the first dose vaccinated individuals $V(t)$ and the protected population $P(t)$ in system (2.1).

The structure of this paper is organized as follows: In the second section, we establish a rubella disease model, denoted as SVPEAIRS, to describe the transmission dynamics of periodic infectious diseases and verify the positive invariance of the system. Then, we define the basic reproduction number and study the threshold theory of global dynamics in the third section. Finally, in the fourth section, by numerical simulation of rubella cases in China, we verify the theoretical results.

2. Mathematical modeling

In this section, we explore a key aspect in the epidemiology of rubella, namely the seasonal fluctuations in rubella. In order to more accurately understand and predict the epidemic trend of rubella, we construct an SVPEAIRS model that considers the periodicity of time. The model not only reflects the seasonal variation of rubella patients, but also takes into account the incubation period of the disease and the impact of vaccination policies.

In order to more accurately simulate the transmission and control effect of rubella in different populations, we divide the rubella population into seven different subcategories. These

compartments include

- Susceptible individuals $S(t)$.
- Exposed individuals $E(t)$ who are exposed to the virus but not diagnosed for rubella yet.
- Symptomatic infected individuals $I(t)$, with clinical symptoms, including fever, rash, lymphadenopathy, etc.
- Asymptomatic infected individuals $A(t)$, no clinical symptoms.
- The first dose vaccinated individuals $V(t)$ who have received the first dose of the MMR vaccine.
- Protected individuals $P(t)$ who have received the second dose of MMR vaccine and have active immunity.
- Recovering individuals $R(t)$ who have temporarily acquired immunity.

Therefore, the transmission process of rubella can be described by the following seven differential equations

$$\begin{cases} \dfrac{\mathrm{d}S}{\mathrm{d}t} = \Lambda + \rho R + fV - \beta(t)S(I + c_1E + c_2A) - (\sigma + \mu)S, \\ \dfrac{\mathrm{d}E}{\mathrm{d}t} = \beta(t)S(I + c_1E + c_2A) - (m + \mu)E, \\ \dfrac{\mathrm{d}A}{\mathrm{d}t} = (1 - q)mE - (r_2 + \mu + b)A, \\ \dfrac{\mathrm{d}I}{\mathrm{d}t} = qmE - (r_1 + \mu + b)I, \\ \dfrac{\mathrm{d}R}{\mathrm{d}t} = r_1I + r_2A - (\rho + \mu)R, \\ \dfrac{\mathrm{d}V}{\mathrm{d}t} = \sigma S - (f + \delta + \mu)V, \\ \dfrac{\mathrm{d}P}{\mathrm{d}t} = \delta V - \mu P, \end{cases} \tag{2.1}$$

where the parameters are shown in Table 1. The model is developed under the following assumptions:

- Susceptible individuals are exposed to rubella after exposure to respiratory droplets of people infected with rubella.
- Exposed individuals can infect others.
- Individuals infected with rubella may recover or die.
- Individuals who have been vaccinated once may lose all immunity and become susceptible, the possibility of these individuals becoming infected is not considered in our analysis.
- Individuals who receive two doses of the MMR vaccine develop active immunity.
- All parameters used in this system are positive.

Table 1. Descriptions of parameters in model (2.1).

Parameters	Description
Λ	Recruitment rate for humans
μ	Natural mortality rate of humans
$\beta(t)$	Basic transmission rate between a susceptible and a symptomatic individual
c_1	Modification factor of transmission rate for exposed individuals
c_2	Modification factor of transmission rate for asymptomatic individuals
q	Proportion of the exposed developing infected with symptoms
m	Transfer rate from exposed to infectious
r_1	Recovery rate of symptomatic infected individuals
r_2	Recovery rate of asymptomatic infected individuals
ρ	Lose of temporary immunity rate
b	Mortality rate due to disease
σ	First dose vaccination rate
f	Waning out of first vaccination rate
δ	Second dose vaccination rate

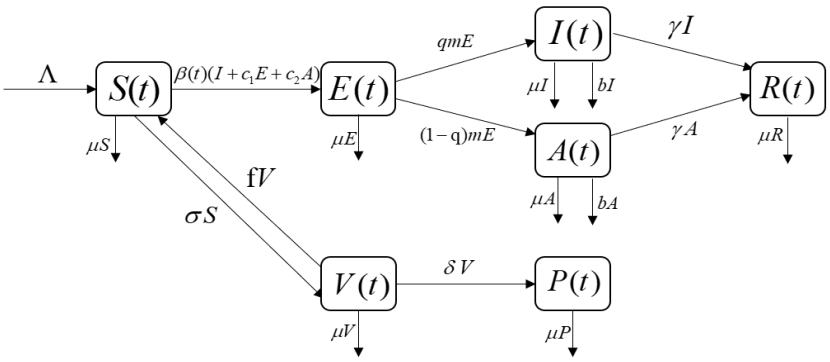

Figure 1. Schematic flow diagram for the rubella model (2.1).

Assume that the total number is $N(t) = S(t) + E(t) + I(t) + A(t) + V(t) + P(t) + R(t)$ and we know that rubella virus is infectious during the incubation period. Based on the above population classification and model assumptions, a detailed schematic is shown in Figure 1.

Because rubella transmission is influenced by climate, social activities, and population movements, leading to seasonal variations in infection rates, the introduction of a periodic transmission rate $\beta(t)$ can improve model accuracy and support effective public health intervention strategies. We assume that $\beta(t)$ is a continuous, positive periodic function with period ω ($\omega > 0$). To capture seasonal patterns, $\beta(t)$ is commonly modeled as:

$$\beta(t) = \beta_0(1 + b\cos(\tfrac{2\pi}{\omega}t + \phi)),$$

which represents the transmission rate from symptomatic individuals to susceptible individuals [23].

In view of the biological interpretations, we denote

$$G := \left\{ (S, V, P, E, A, I, R) \in \mathbb{R}^7 | 0 \leq S + V + P + E + A + I + R \leq \frac{\Lambda}{\mu} \right\}.$$

Lemma 2.1. *G is the positive invariant set of the system* (2.1).

Proof. By system (2.1), we can get $\frac{\mathrm{d}N}{\mathrm{d}t} = \Lambda - \mu N - b(I + A) \leq \Lambda - \mu N$. For the equation $\frac{\mathrm{d}\bar{N}}{\mathrm{d}t} = \Lambda - \mu\bar{N}$ under the initial condition $\bar{N}(t_0)$, we have

$$\bar{N}(t) = \frac{\Lambda}{\mu} + \bar{N}(t_0)e^{-\mu(t-t_0)},$$

furthermore, $\lim\limits_{t\to\infty} \bar{N}(t) = \frac{\Lambda}{\mu}$. It follows from the comparison principle that $N(t) \leq \frac{\Lambda}{\mu}$, so G is the positive invariant set of the system (2.1). □

Let $z(t)$ be a matrix-valued function of a period of order $n \times n$, and it is continuous, cooperative, irreducible, and its period is ω. $\phi_z(t)$ is defined as a monodromy matrix of linear ordinary differential equation

$$x' = z(t)x,$$

and $r(\phi_z(t))$ is the spectral radius of $\phi_z(t)$.

In the study of dynamic system stability, the asymptotic and periodic properties of solutions are crucial. Lemma 2.2 decomposes the solution into an exponentially growing term and a periodically modulated term, establishes the relationship between system dynamics and parameters, and provides an explicit solution expression. This not only facilitates calculations but also serves as a key support for subsequent theoretical derivations.

Lemma 2.2 (Lemma 2.1, [23]). *Let $z(t)$ be a continuous, cooperative, irreducible, and ω-periodic $n \times n$ matrix function. Let $\phi_z(\omega)$ be the monodromy matrix of the linear ω-periodic system*

$$x' = z(t)x,$$

and denote by $r(\phi_z(\omega))$ its spectral radius. Define $\varphi = \frac{1}{\omega}\ln r(\phi_z(\omega))$. Then there exists a positive ω-periodic function $\nu(t)$ such that

$$e^{\varphi t}\nu(t)$$

is a solution to the system $x' = z(t)x$.

3. Threshold dynamics

In this section, we first define the basic reproduction number $\mathcal{R}_0$ of the system (2.1), and then discuss the extinction and uniform persistence of the disease.

With simple calculations, we determine that the system (2.1) has a disease-free equilibrium $\mathcal{M}_0 = (S_0, 0, 0, 0, 0, V_0, P_0)$, where

$$S_0 = \frac{\Lambda(f + \delta + \mu)}{(\sigma + \mu)(f + \delta + \mu) - f\delta},$$
$$V_0 = \frac{\Lambda\sigma}{(\sigma + \mu)(f + \delta + \mu) - f\delta},$$

$$P_0 = \frac{\Lambda\sigma\delta}{((\sigma+\mu)(f+\delta+\mu)-f\delta)\mu}.$$

According to the classification of [18], the system compartment is rearranged as $x = (x_1, x_2, x_3, x_4, x_5, x_6, x_7)^\top$, where the infected compartments is $(x_1, x_2, x_3) = (E, A, I)$, and the uninfected chamber is $(x_4, x_5, x_6, x_7) = (S, R, V, P)$.

Define $X_S := \{x \geq 0 : x_i = 0, \forall i = 1, 2, 3\}$ as the set of all disease-free states, and the system (2.1) has a disease-free periodic solution $x^0(t)$, then define

$\mathcal{F}_i(t, x)$: Entry rate of newly infected individuals in compartment i;

$\mathcal{V}_i^+(t, x)$: The rate of entry by other means (for example, birth rate, immigration rate) of individuals in compartment i;

$\mathcal{V}_i^-(t, x)$: The rate of individual output (for example, mortality, recovery rate, immigration rate) in compartment i.

Thus, the periodic infectious disease model is controlled by a non-autonomous ordinary differential system:

$$x_i'(t, x) = \mathcal{F}_i(t, x) - \mathcal{V}_i(t, x) \triangleq f_i(t, x), \ i = 1, 2, \cdots 7,$$

where $\mathcal{V}_i(t, x) = \mathcal{V}_i^-(t, x) - \mathcal{V}_i^+(t, x)$. The system (2.1) can be written as

$$x' = \mathcal{F} - \mathcal{V},$$

where

$$\mathcal{F} = \begin{pmatrix} \beta(t)S(I + c_1E + c_2A) \\ 0 \\ 0 \\ 0 \\ 0 \\ 0 \\ 0 \end{pmatrix},$$

$$\mathcal{V} = \begin{pmatrix} (m+\mu)E \\ (r_2+\mu+b)A - (1-q)mE \\ (r_1+\mu+b)I - qmE \\ \beta(t)S(I + c_1E + c_2A) + (\sigma+\mu)S - (\Lambda + \rho R + fV) \\ (\rho+\mu)R - (r_1I + r_2A) \\ (f+\delta+\mu)V - \sigma S \\ \mu P - \delta V \end{pmatrix}.$$

Further, we can get $D\mathcal{F}(t,x^0(t)) = \begin{pmatrix} F(t) & 0 \\ 0 & 0 \end{pmatrix}$ and $D\mathcal{V}(t,x^0(t)) = \begin{pmatrix} V(t) & 0 \\ J(t) & -M(t) \end{pmatrix}$, where

$$F(t) = \begin{pmatrix} c_1\beta(t)S_0 & c_2\beta(t)S_0 & \beta(t)S_0 \\ 0 & 0 & 0 \\ 0 & 0 & 0 \end{pmatrix}$$

and

$$V(t) = \begin{pmatrix} m+\mu & 0 & 0 \\ -(1-q)m & r_2+\mu+b & 0 \\ -qm & 0 & r_1+\mu+b \end{pmatrix}.$$

Let $Y(t,s), t \geq s$, be the evolution operator of the linear ω-periodic system $y'(t) = -V(t)y(t)$, namely for any $s \in \mathbb{R}$, the 3×3 matrix $Y(t,x)$ satisfies

$$\frac{\partial Y(t,s)}{\partial t} = -V(t)Y(t,x), \forall t \geq s, Y(s,s) = I,$$

where I is the 3×3 identity matrix.

Now, we derive the basic reproduction number $\mathcal{R}_0$ for model (2.1) by following the general calculation method presented in [18], we introduce a linear periodic system

$$z'(t) = \left(-V(t) + \frac{F(t)}{\lambda}\right) z, t \in \mathbb{R}, \tag{3.1}$$

with parameter $\lambda > 0$. Let $W(t,s,\lambda), t \geq s, s \in \mathbb{R}$ be the evolution operator of the system (2.1) on $C(\mathbb{R}^3)$, obviously, $\phi_{F-V}(t) = W(t,0,1), \forall t \geq 0$.

Let C_ω be the ordered Banach space of all ω-periodic functions from $\mathbb{R} \to \mathbb{R}^3$ with the maximum norm $\|\cdot\|$. Let C_ω^+ be the positive cone $\{\phi \in C_\omega : \phi(t) \geq 0, \forall t \in \mathbb{R}\}$. Following [18], we define a linear operator $L : C_\omega \to C_\omega$ as follows:

$$(L\phi)(t) = \int_0^\infty Y(t,t-a)F(t-a)\phi(t-a)da.$$

The operator L can be called the next infection operator and the spectral radius of L can be defined as the basic reproduction number for system (2.1), that is

$$\mathcal{R}_0 := r(L).$$

Thus, we have the following results.

Lemma 3.1 (Theorem 2.1, [18]). *The following statements are valid:*

(i) If $r(W(\omega,0,\lambda)) = 1$ has a positive root λ_0, then λ_0 is an eigenvalue of L, and hence $\mathcal{R}_0 > 0$.

(ii) If $\mathcal{R}_0 > 0$, then $\lambda = \mathcal{R}_0$ is the unique root of $r(W(\omega,0,\lambda)) = 1$.

(iii) $\mathcal{R}_0 = 0$ *if and only if* $r(W(\omega, 0, \lambda)) < 1, \forall \lambda > 0$.

Hence, we know $\mathcal{R}_0$ is the unique solution of $r(W(\omega, 0, \lambda)) = 1$, then the basic reproduction number $\mathcal{R}_0$ can be estimated by the numerical solution of the equation. Regarding the local stability of the system (2.1) at the disease-free equilibrium W_0, we have the following results.

Lemma 3.2 (Theorem 2.1, [18]). *The following assertions are valid.*

(i) $\mathcal{R}_0 = 1$ *if and only if* $r(\phi_{F-V}(\omega)) = 1$.

(ii) $\mathcal{R}_0 > 1$ *if and only if* $r(\phi_{F-V}(\omega)) > 1$.

(iii) $\mathcal{R}_0 < 1$ *if and only if* $r(\phi_{F-V}(\omega)) < 1$.

Therefore, the disease-free equilibrium $\mathcal{M}_0$ of system (2.1) is locally asymptotically stable at $\mathcal{R}_0 < 1$ and unstable at $\mathcal{R}_0 > 1$, where $\phi_{F-V}(\omega)$ is the monodromy matrix of a linear ω-periodic system.

In the special case where $\beta(t) \equiv \beta$, for all $t \geq 0$, we find that $F(t) \equiv F$. Using the results from [5] and [18, Lemma 2.2(ii)], we can derive the expression for the basic reproduction number $[\mathcal{R}_0]$ for the autonomous system described in system (2.1)

$$[\mathcal{R}_0] = \frac{\beta\Lambda(f+\delta+\mu)}{((\sigma+\mu)(f+\delta+\mu)+f\delta)(m+\mu)}\left(c_1 + \frac{c_2(1-q)m}{r_2+\mu+b} + \frac{qm}{r_1+\mu+b}\right).$$

We now define the effective reproduction number for the system (2.1).

Definition 3.1. The effective reproduction number at time t is

$$[\mathcal{R}_0] = \frac{\beta\Lambda(f+\delta+\mu)}{((\sigma+\mu)(f+\delta+\mu)+f\delta)(m+\mu)}\left(c_1 + \frac{c_2(1-q)m}{r_2+\mu+b} + \frac{qm}{r_1+\mu+b}\right).$$

Theorem 3.1. *For any solution of the system* (2.1)*, if* $\mathcal{R}_0 < 1$*, then the disease-free equilibrium* $\mathcal{M}_0$ *is globally asymptotically stable; if* $\mathcal{R}_0 > 1$*, then it is unstable.*

Proof. When $\mathcal{R}_0 < 1$, the local stability of $\mathcal{M}_0$ and $\mathcal{R}_0 > 1$ is unstable are known from Lemma 3.2, and now we need to prove the global attractive of system (2.1).

Let $B_\eta(t) = F_\eta(t) - V(t)$, where

$$F_\eta(t) = \begin{pmatrix} c_1\beta(t)(S_0+\eta) & c_2\beta(t)(S_0+\eta) & \beta(t)(S_0+\eta) \\ 0 & 0 & 0 \\ 0 & 0 & 0 \end{pmatrix}.$$

According to the Lemma 3.2, it can be known that when $\mathcal{R}_0 < 1$, $r(\phi_{F-V}(\omega)) < 1$, now choose $\eta > 0$ sufficiently small to satisfy $r(\phi_{B_\eta}(\omega)) < 1$.

Since $\mathcal{M}_0$ is locally stable, when $\mathcal{R}_0 < 1$, for any $\eta > 0$, there exists a $t_1 > 0$, such that $S(t) \leq S_0 + \eta$, for all $t \geq t_1$.

Thus,

$$\begin{cases} \dfrac{\mathrm{d}E}{\mathrm{d}t} \leq \beta(t)(S_0+\eta)(I + c_1E + c_2A) - (m+\mu)E, \\ \dfrac{\mathrm{d}A}{\mathrm{d}t} \leq (1-q)mE - (r_2+\mu+b)A, \\ \dfrac{\mathrm{d}I}{\mathrm{d}t} \leq qmE - (r_1+\mu+b)I. \end{cases}$$

Consider a auxiliary system

$$\begin{cases} \dfrac{\mathrm{d}\bar{E}}{\mathrm{d}t} = \beta(t)(S_0+\eta)(\bar{I}+c_1\bar{E}+c_2\bar{A}) - (m+\mu)\bar{E}, \\ \dfrac{\mathrm{d}\bar{A}}{\mathrm{d}t} = (1-q)m\bar{E} - (r_2+\mu+b)\bar{A}, \\ \dfrac{\mathrm{d}\bar{I}}{\mathrm{d}t} = qm\bar{E} - (r_1+\mu+b)\bar{I}. \end{cases} \tag{3.2}$$

Since system (3.2) satisfies the conditions specified in Lemma 2.2, there exists a positive ω-period function $v(t) = (v_1(t), v_2(t), v_3(t))^{\mathrm{T}}$. Consequently, the function $e^{\varphi_1 t}v(t)$ is a solution of system (3.1), where $\varphi_1 = \frac{1}{\omega}\ln(r(\phi_{B_\eta}(\omega))) < 0$. By choosing $t_2 > t_1$ and a sufficiently small positive value $\xi > 0$, the following inequalities hold:

$$\bar{E}(t_2) \le \xi v_1(0), \bar{A}(t_2) \le \xi v_2(0), \bar{I}(t_2) \le \xi v_3(0).$$

When $t > t_2$,

$$\begin{cases} \bar{E}(t) \le \xi e^{\varphi_1(t-t_1)}v_1(t-t_2), \\ \bar{A}(t) \le \xi e^{\varphi_1(t-t_1)}v_2(t-t_2), \\ \bar{I}(t) \le \xi e^{\varphi_1(t-t_1)}v_3(t-t_2). \end{cases}$$

According to the comparison principle, when $t > t_2$, we have $E(t) \le \bar{E}(t), A(t) \le \bar{A}(t), I(t) \le \bar{I}(t)$. Since $\varphi_1 < 0$, it can be proven that

$$\lim_{t\to\infty} E(t) = 0, \lim_{t\to\infty} A(t) = 0, \lim_{t\to\infty} I(t) = 0.$$

Furthermore, according to the limit system theory, it is easy to verify

$$\begin{aligned} &\lim_{t\to\infty} S(t) = \frac{\Lambda(f+\delta+\mu)}{(\sigma+\mu)(f+\delta+\mu)+f\delta}, \\ &\lim_{t\to\infty} V(t) = \frac{\Lambda\sigma}{(\sigma+\mu)(f+\delta+\mu)+f\delta}, \\ &\lim_{t\to\infty} P(t) = \frac{\Lambda\sigma\delta}{((\sigma+\mu)(f+\delta+\mu)+f\delta)\mu}, \\ &\lim_{t\to\infty} R(t) = 0. \end{aligned}$$

Therefore, $\mathcal{M}_0$ is globally attractive. Further, $\mathcal{M}_0$ is globally asymptotically stable. □

Theorem 3.2. *When $\mathcal{R}_0 > 1$, the system (2.1) is uniformly persistent, namely, there exists a positive constant $\eta > 0$, such that any solution $(S(t), V(t), P(t), E(t), A(t), I(t), R(t))$ in G of system (2.1) with $E(0) > 0$ or $A(0) > 0$ or $I(0) > 0$ satisfies*

$$\liminf_{t\to\infty} E(t) \ge \eta, \quad \liminf_{t\to\infty} A(t) \ge \eta, \quad \liminf_{t\to\infty} I(t) \ge \eta.$$

Proof. Define $X := G$, $X_0 := \{(S, E, A, I, R, V, P) \in X : E > 0, A > 0, I > 0\}$, $\partial X_0 := X \backslash X_0$. Obviously, X_0 and ∂X_0 are positively invariant, and ∂X_0 is a relatively closed set of X. Let $J : X \to X$ be the Poincaré map of system (2.1), defined by $J(x^0) = u(\omega, x^0)$, where $u(t, x^0)$

denotes the unique solution of system (2.1) with the initial condition $u(0,x^0)=x^0$. Here, $x^0=(S^0,E^0,A^0,I^0,R^0,V^0,P^0)\in X_0$ and $u(t,x^0)=(S(t,x^0),E(t,x^0),A(t,x^0),I(t,x^0),R(t,x^0),V(t,x^0),P(t,x^0))$.

Next, we will prove that $W^s(\mathcal{M}_0)\cap X_0=\emptyset$, where $W^s(\mathcal{M}_0)$ represents the stable set of $\mathcal{M}_0$ for the mapping J.

By the continuity of solutions on initial values, we have $\lim\limits_{x^0\to\mathcal{M}_0}\parallel \mathrm{u}(t,x^0)-\mathcal{M}_0\parallel=0$ for $t\in[0,\omega]$, where the symbol $\|\cdot\|$ represents the Euclidean distance on $\mathbb{R}^7$, then $\forall\varepsilon>0,\exists\delta_0=\delta_0(\varepsilon)>0$, such that when $\parallel x^0-\mathcal{M}_0\parallel\le\delta_0$, we have

$$\parallel u(t,x^0)-\mathcal{M}_0)\parallel<\varepsilon,\forall t\in[0,\omega].$$

We claim that $\limsup\limits_{m\to\infty}\parallel J^m(x^0)-\mathcal{M}_0\parallel\ge\delta_0$ is valid for any $x^0\in X_0$. Otherwise, there exists $\bar{x}^0\in X_0$, such that

$$\limsup_{m\to\infty}\parallel J^m(\bar{x}^0)-\mathcal{M}_0\parallel<\delta_0.$$

Then, it can be assumed that for $\forall m>m_0$ where $m_0\in\mathbb{N}$, there is $\parallel J^m(\bar{x}^0)-\mathcal{M}_0\parallel<\delta_0$, therefore, $\forall t\in[0,\omega]$ there is

$$\parallel u(t,J^m(\bar{x}^0))-\mathcal{M}_0)\parallel<\varepsilon.$$

For any $t\ge m_0\omega$, we have $t=n\omega+t_1$, $t_1\in[0,\omega)$, where $n=\left[\frac{t}{\omega}\right]$ denotes the largest integer not greater than $\frac{t}{\omega}$ and $n\ge m_0$. Then

$$\parallel u(t,\bar{x}^0)-\mathcal{M}_0)\parallel=\parallel u(t_1,J^n(\bar{x}^0))-\mathcal{M}_0)\parallel<\varepsilon.$$

Therefore when $t\ge m_0\omega$, there is $0<E(t,\bar{x}^0),A(t,\bar{x}^0),I(t,\bar{x}^0),R(t,\bar{x}^0)<\varepsilon$, and

$$\begin{aligned}
&\left|S(t,\bar{x}^0)-\frac{\Lambda(f+\delta+\mu)}{(\sigma+\mu)(f+\delta+\mu)+f\delta}\right|<\varepsilon,\\
&\left|V(t,\bar{x}^0)-\frac{\Lambda\sigma}{(\sigma+\mu)(f+\delta+\mu)+f\delta}\right|<\varepsilon,\\
&\left|P(t,\bar{x}^0)-\frac{\Lambda\sigma\delta}{((\sigma+\mu)(f+\delta+\mu)+f\delta)\mu}\right|<\varepsilon.
\end{aligned}$$

Substituting into system (2.1), we find that when $t\ge m_0\omega$, the functions $E(t,\bar{x}^0),A(t,\bar{x}^0),I(t,\bar{x}^0)$ satisfiy the following inequalities

$$\begin{cases}
\dfrac{\mathrm{d}E}{\mathrm{d}t}\ge\beta(t)(S_0-\varepsilon)(I+c_1E+c_2A)-(m+\mu)E,\\
\dfrac{\mathrm{d}A}{\mathrm{d}t}\ge(1-q)mE-(r_2+\mu+b)A,\\
\dfrac{\mathrm{d}I}{\mathrm{d}t}\ge qmE-(r_1+\mu+b)I.
\end{cases}$$

Consider a auxiliary system as follows

$$\begin{cases}
\dfrac{\mathrm{d}\hat{E}}{\mathrm{d}t}=\beta(t)(S_0-\varepsilon)(\hat{I}+c_1\hat{E}+c_2\hat{A})-(m+\mu)\hat{E},\\
\dfrac{\mathrm{d}\hat{A}}{\mathrm{d}t}=(1-q)m\hat{E}-(r_2+\mu+b)\hat{A},\\
\dfrac{\mathrm{d}\hat{I}}{\mathrm{d}t}=qm\hat{E}-(r_1+\mu+b)\hat{I}.
\end{cases}\tag{3.3}$$

Set $C_\varepsilon(t) = F_\varepsilon(t) - V(t)$, where

$$F_\varepsilon(t) = \begin{pmatrix} c_1\beta(t)(S_0-\varepsilon) & c_2\beta(t)(S_0-\varepsilon) & \beta(t)(S_0-\varepsilon) \\ 0 & 0 & 0 \\ 0 & 0 & 0 \end{pmatrix}.$$

Since $\mathcal{R}_0 > 1$, it follows that $r(\phi_{F-V}(\omega)) > 1$. We can choose a sufficiently small $\varepsilon > 0$ such that $r(\phi_{C_\varepsilon}(\omega)) > 1$. By Lemma 2.2, there exists an ω-periodic function $p(t) = (p_1(t), p_2(t), p_3(t))^\top \geq 0$ such that $e^{\varphi_2 t}p(t)$ is the solution to the system (3.3), where $\varphi_2 = \frac{1}{\omega}\ln(r(\phi_{C_\varepsilon}(\omega))) > 0$. Next, we choose $\alpha > 0$ such that

$$(E(m_0\omega, \bar{x}_0), A(m_0\omega, \bar{x}_0), I(m_0\omega, \bar{x}_0)) \geq \alpha(\hat{E}(m_0\omega), \hat{A}(m_0\omega), \hat{I}(m_0\omega)).$$

By the comparison principle, it follows that

$$(E(t, \bar{x}^0), A(t, \bar{x}^0), I(t, \bar{x}^0)) \geq \alpha(\hat{E}(t), \hat{A}(t), \hat{I}(t))$$

for $t \geq m_0\omega$. Therefore, we obtain

$$\lim_{m\to\infty} E(m\omega, \bar{x}_0) = \infty, \ \lim_{m\to\infty} A(m\omega, \bar{x}_0) = \infty, \ \lim_{m\to\infty} I(m\omega, \bar{x}_0) = \infty,$$

which leads to a contradiction. Thus, we conclude that $\limsup_{m\to\infty} \mathrm{d}(\mathrm{J}^{\mathrm{m}}(\mathrm{x}^0), \mathcal{M}_0) \geq \delta_0$. Therefore, $\mathcal{M}_0$ is an isolated invariant set for the Poincaré mapping J in X, and we have $W^s(\mathcal{M}_0) \cap X_0 = \emptyset$.

Let

$$\begin{aligned} M_\partial = &\{(S^0, E^0, A^0, I^0, R^0, V^0, P^0) \in \partial X_0 \\ &\big| J^m(S^0, E^0, A^0, I^0, R^0, V^0, P^0) \in \partial X_0, \forall m \in \mathbb{N}\}. \end{aligned}$$

We will prove that $M_\partial = \{(S, 0, 0, 0, R, V, P) : S \geq 0, R \geq 0, V \geq 0, P \geq 0\}$.

It is easy to know that $\{(S, 0, 0, 0, R, V, P) : S \geq 0, R \geq 0, V \geq 0, P \geq 0\} \subseteq M_\partial$. Therefore it only needs to prove that

$$M_\partial \subseteq \{(S, 0, 0, 0, R, V, P) : S \geq 0, R \geq 0, V \geq 0, P \geq 0\},$$

namely, we need to prove that for any $x^0 \in M_\partial$, the solution $u(t, x^0)$ through $(0, x^0)$ satisfies $E(t, x^0) = A(t, x^0) = I(t, x^0) = 0$ for all $t \geq 0$.We use proof by contradiction. Assume that there exists a $\bar{t} > 0$, such that $E(\bar{t}, x^0) > 0$ or $A(\bar{t}, x^0) > 0$ or $I(\bar{t}, x^0) > 0$. Without loss of generality, we verify one case $A(\bar{t}, x^0) > 0$, the other cases can be proven similarly.

From system (2.1), we have $A'(t) \geq -(r_2 + \mu + b)A$, which implies that $A(t, x^0) > 0$ for $t \geq \bar{t}$. Further, we have

$$E(t, x^0) \geq (E(\bar{t}, x^0) + \int_{\bar{t}}^{t} c_2\beta(\xi)A(\xi, x^0)e^{(m+\mu)\xi}d\xi)e^{-(m+\mu)t} > 0,$$

and

$$I(t, x^0) \geq (I(\bar{t}, x^0) + \int_{\bar{t}}^{t} qmE(\xi)e^{(r_1+\mu+b)\xi}d\xi)e^{-(r_1+\mu+b)t} > 0$$

for all $t > \bar{t}$.

We conclude that $E(t, x^0) > 0, A(t, x^0) > 0, I(t, x^0) > 0$ for all $t > \bar{t}$, which means $u(t, x^0) \in X_0$ for $t > \bar{t}$, contrary to $x^0 \in M_\partial$. In summary, it is concluded that

$$M_\partial = \{(S, 0, 0, 0, R, V, P) : S \geq 0, R \geq 0, V \geq 0, P \geq 0\}.$$

Then, we prove that $\omega(x^0) = \{\mathcal{M}_0\}$, where $\omega(x^0)$ is the omega limit set of the forward orbit $\gamma^+(x^0) = \{J^m(x^0) : \forall m \in \mathbb{N}\}$ of system (2.1). Since

$$M_\partial = \{(S, 0, 0, 0, R, V, P) : S \geq 0, R \geq 0, V \geq 0, P \geq 0\},$$

we have $E(t, x^0) = 0, A(t, x^0) = 0, I(t, x^0) = 0$. And by the system (2.1), we consider the following system

$$\begin{cases} \dfrac{\mathrm{d}S}{\mathrm{d}t} = \Lambda + \rho R + \omega V - (\sigma + \mu)S, \\ \dfrac{\mathrm{d}R}{\mathrm{d}t} = -(\rho + \mu)R, \\ \dfrac{\mathrm{d}V}{\mathrm{d}t} = \sigma S - (f + \delta + \mu)V, \\ \dfrac{\mathrm{d}P}{\mathrm{d}t} = \delta V - \mu P. \end{cases} \tag{3.4}$$

From the system (3.4), we have $\lim\limits_{t\to\infty}(S(t) - S_0, R(t), V(t) - V_0, P(t) - P_0) = (0, 0, 0, 0)$. Therefore $\omega(x^0) = \{\mathcal{M}_0\}$ for all $x^0 \in M_\partial$, and it is easy to prove that $\mathcal{M}_0$ is a global attractor for the mapping J in M_∂. Since the system (3.4) is cooperative, by [22, Lemma 2.2.1], we have $\mathcal{M}_0$ is Lyapunov stable for the mapping J in M_∂. Therefore $\mathcal{M}_0$ is globally stable for the mapping J in M_∂. Based on the above proof, we know that $\cup_{x^0 \in M_\partial}\omega(x^0) = \mathcal{M}_0$ and $\mathcal{M}_0$ cannot form a cycle for the mapping J in M_∂ and ∂X_0. Since all solutions are ultimately bounded [9, Theorem 2.1], J has a global attractor on X. According to [22, Theorem 1.3.1] and [22, Remark 1.3.1], we conclude that the mapping $J : X \to X$ is uniformly persistent with respect to $(X_0, \partial X_0)$.

Consequently, it follows from the conclusions of [22, Theorem 3.1.1] and [9, Lemma 3.3] that the solution of system (2.1) is uniformly persistent under $E(0) > 0$ or $A(0) > 0$ or $I(0) > 0$. □

Theorem 3.3. *If $\mathcal{R}_0 > 1$, the system (2.1) admits at least one positive ω-periodic solution*

$$(S^*(t), E^*(t), A^*(t), I^*(t), R^*(t), V^*(t), P^*(t)),$$

where all components are strictly positive for all $t \geq 0$.

Proof. According to Theorem 3.2 and [22, Theorem 1.3.10]), the Poincaré map J has a fixed point $(S^*(0), E^*(0), A^*(0), I^*(0), R^*(0), V^*(0), P^*(0)) \in X_0$. The corresponding periodic solution is represented as $(S^*(t), E^*(t), A^*(t), I^*(t), R^*(t), V^*(t), P^*(t))$. Since $E^*(0) > 0$,$I^*(0) > 0$ and $A^*(0) > 0$, it follows that $E^*(t) > 0, I^*(t) > 0, A^*(t) > 0$ for all $t \geq 0$. Furthermore, integrating the fifth equation from the system (2.1), yields

$$R^*(t) = (R^*(0) + \int_0^t (r_1 I^*(\xi) + r_2 A^*(\xi))e^{(\rho+\mu)\xi} d\xi)e^{-(\rho+\mu)t} > 0$$

for all $t > 0$. The periodicity of $R^*(t)$ implies $R^*(t) > 0$ for all $t \geq 0$. Similarly, we can conclude that $S^*(t) > 0, V^*(t) > 0, P^*(t) > 0$ for all $t \geq 0$.

Therefore, $(S^*(t), E^*(t), A^*(t), I^*(t), R^*(t), V^*(t), P^*(t))$ is a positive ω-periodic solution of the system (2.1). □

4. Numerical simulations

4.1. Model application

In the above theoretical analysis, we show that the basic reproduction number $\mathcal{R}_0$ is a critical threshold parameter for determining whether the disease becomes epidemic or not. The section validate this conclusion by numerical simulations. The initial state values for system (2.1) are set as follows: $S_0 = 1260\ 000$, $E_0 = 9\ 000$, $A_0 = 7\ 956$, $I_0 = 1\ 326$, $R_0 = 0$, $V_0 = 0$, $P_0 = 0$, and the values of the parameters are showed in Table 2.

Table 2. Parameters and their values in model (2.1).

Parameters	Value	Source
Λ	1500000	China Statistical Yearbook
μ	0.0059	China Statistical Yearbook
c_1	0.02	Assumed
c_2	0.08	Assumed
q	0.5	Assumed
m	0.1	Assumed
r_1	0.6	Assumed
r_2	0.7	Assumed
ρ	0.01	[17]
b	0.08	[17]
σ	0.3	[17]
f	0.6	[17]
δ	0.8	Assumed

A periodic function is selected as $\beta(t) = \beta_0(1 + b\cos(\frac{\pi}{6}t + \phi)$, with $\omega = 12$. For the numerical simulation, we collect reported cases of rubella in China from January 2012 to December 2018, where the data source is the Public Health Sciences Data Center, see Figure 2.

Using MATLAB, the least squares method yields the following estimates: $\beta_0 = 3.2972 \times 10^{-9}, b = -2.5966, \phi = 2.5022$ and $\mathcal{R}_0 = 0.9367$. According to Theorem 3.4, this indicates that the disease will eventually extinct. Figure 3 presents the results of the numerical simulation, which corroborate this conclusion.

Furthermore, if the recovery rates of symptomatic infected and asymptomatic infected people are adjusted: $r_1 = 0.3$, $r_2 = 0.35$ while keeping the initial system values and other parameters remain unchanged, the calculation result is $\mathcal{R}_0 = 1.8856$. If the vaccination rate of the first and second doses are adjusted: $\sigma = 0.15$, $\delta = 0.4$ while keeping the initial system values and other parameters remain unchanged, the calculation result is $\mathcal{R}_0 = 2.0152$. According to Theorems 3.2 and 3.3 when $\mathcal{R}_0 > 1$, the system (2.1) demonstrates uniform persistence, and there exists

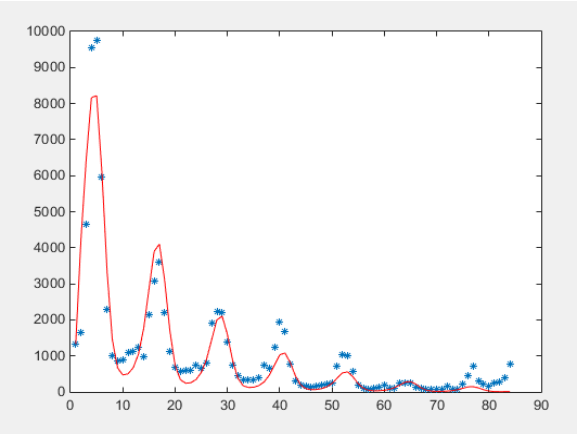

Figure 2. Comparison of reported cases of rubella in China from January 2012 to December 2018 and model (2.1) simulations, where time 0 represents January 1th, 2012, until December 31th, 2018.

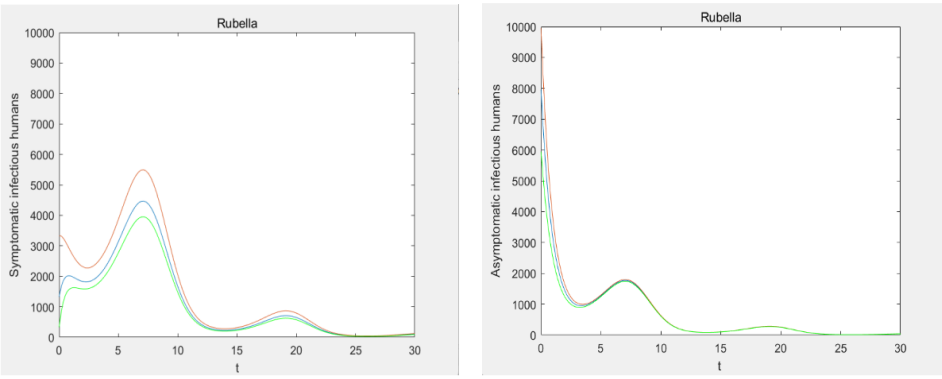

Figure 3. When $\mathcal{R}_0 = 0.9367$, the trend of symptomatic infectious humans and asymptomatic infectious humans.

a positive ω-periodic solution for system (2.1). Figure 4 presents the results of a numerical simulation of the reduced recovery rate. Figure 5 presents the results of a numerical simulation of the reduction in vaccination rates.

After a comprehensive analysis, we clearly point out that once the vaccination rate and recovery rate decline, the epidemic of rubella infectious diseases will become difficult to control, and its spread may become persistent and widespread. This phenomenon underscores the importance of continuing to advance the MMR vaccine program. In order to maintain public health safety, we must take effective measures, such as increasing the vaccination rate of MMR vaccine, so as to effectively prevent the long-term prevalence and spread of rubella infectious diseases.

4.2. Bifurcation phenomenon

Figure 6 illustrates the dynamic behavior of the number of symptomatic and asymptomatic infected individuals as a function of the transmission rate parameter β_0 in system (2.1). Using the amplitude parameter β_0 of the time-varying contact rate $\beta(t) = \beta_0(1 + b\cos(2\pi\omega t + \phi))$ as the bifurcation parameter, we analyze the dynamic phase transitions of the system through numerical simulations. The evolution of the number of symptomatic infected individuals $I(t)$ is

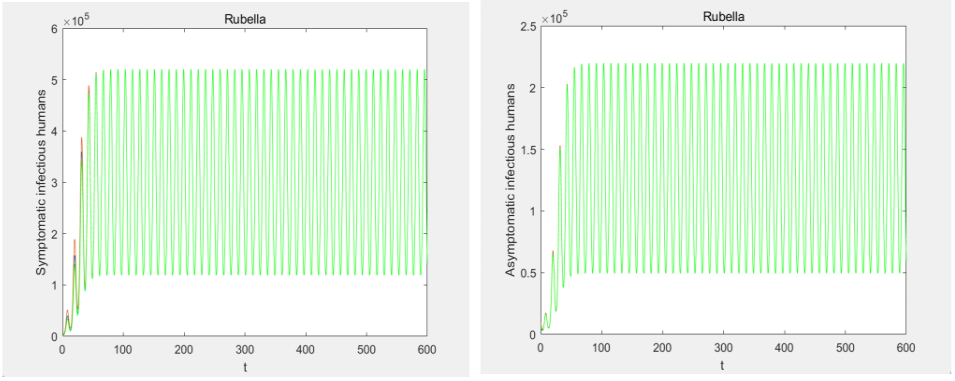

Figure 4. When $\mathcal{R}_0 = 1.8856$, the trend of symptomatic infectious humans and asymptomatic infectious humans.

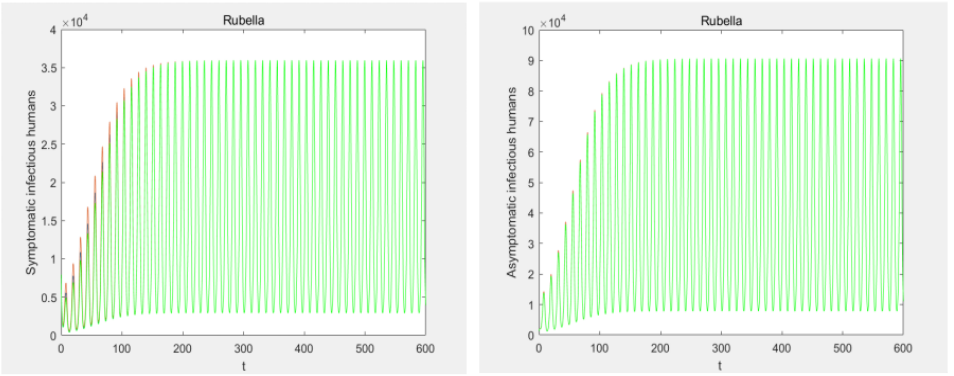

Figure 5. When $\mathcal{R}_0 = 2.0152$, the trend of symptomatic infectious humans and asymptomatic infectious humans.

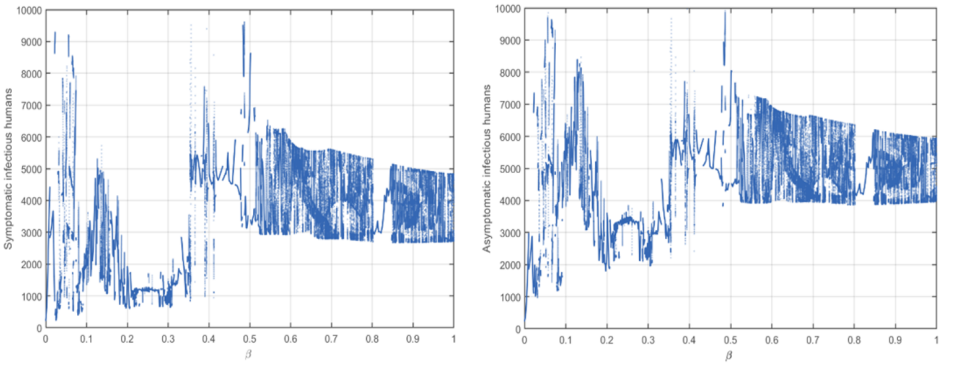

Figure 6. Difurcation diagrams.

shown in Figure 6, while the number of asymptomatic infected individuals $A(t)$ exhibits similar trends. As β_0 increases, the system sequentially displays complex dynamic behaviors such as single-period, chaotic, and stepped behaviors. The detailed analysis is as follows:

(i) **Transient outbreaks and stepped behavior at low infection rates** ($0 < \beta_0 \lesssim 0.1084$):
Within this parameter range, the number of symptomatic infected individuals ($I(t)$) rapidly

peaks and then decays sharply, indicating that the disease cannot sustain itself. At $\beta_0 = 0.0099$, the system exhibits stepped behavior, while a sharp decline in symptomatic infections occurs when the transmission rate increases from 0.0182 to 0.0215.

(ii) **Periodic dynamics at medium infection rates** ($0.2165 \lesssim \beta_0 \lesssim 0.2713$):
The system demonstrates stable single-period motion combined with stepped behavior, with the number of symptomatic infected individuals ($I(t)$) remaining consistently at a low level.

(iii) **Complex dynamics at high infection rates** ($0.3147 \lesssim \beta_0 \lesssim 0.5151$):
Within this parameter range, the system exhibits wide-range stepped behavior. The number of symptomatic infected individuals ($I(t)$) reaches its peak, suggesting a potential strong rebound and sustained transmission of the epidemic in this region. The complex stepped behavior indicates that the system is transitioning toward chaos.

(iv) **Chaos and periodic windows at very high infection rates** ($0.5151 \lesssim \beta_0 \leq 1$):
The system dynamics are chaotic. The number of symptomatic infected individuals ($I(t)$) gradually decreases as β_0 increases. Notably, within the narrow range of $0.8065 \lesssim \beta_0 \lesssim 0.8461$, the system abruptly transitions from chaos to stable single-period motion.

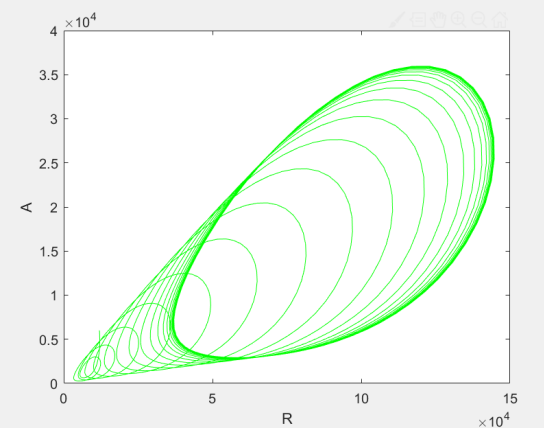

Based on Figure 5, we plot the R-A phase plane diagram, which illustrates the presence of chaotic behavior.

Figure 7. Phase plane diagram.

Bifurcation analysis shows that the rubella transmission system (2.1) is highly sensitive to the transmission rate parameter β_0, and even a slight perturbation may lead to significant changes in the dynamic state of the system; based on the analysis of the impact on transmission dynamics, the following control strategies are proposed: A real-time monitoring and early warning mechanism should be established to ensure that the transmission rate parameter β_0 remains below the high-risk threshold of 0.27, and a special emergency plan targeting chaotic dynamic characteristics needs to be formulated, with particular attention to the periodic windows where the system exhibits short-term regularity, so that strengthening control measures in this phase can effectively mitigate potential epidemic fluctuations.

5. Discussion

The transmission pattern of rubella shows obvious seasonal characteristics. Thus, seasonal and environmental factors need to be considered when constructing models, this adds extra complex-

ity. There are also significant differences in vaccination coverage across areas and populations, this makes it difficult to find uniform parameters and predictions. Additionally, changes in public behavior, such as attitudes towards vaccination, can also affect rubella transmission dynamics, and these changes are often hard to quantify. Finally, the validation and predictive power of models are crucial, accurately predicting changes in rubella cases in a rapidly changing environment is a major challenge.

The study reveals that rubella cases exhibit distinct seasonal patterns, typically peaking between March and June, while maintaining relatively lower incidence rates during winter. This seasonal variation is closely associated with school holidays and family gatherings: Increased social activities during spring and summer facilitate viral transmission, and warmer weather encourages more frequent outdoor gatherings, thereby elevating transmission risks. Although the overall incidence remains lower in winter, localized minor peaks still occur due to prolonged close contact among students in enclosed classrooms, which increases the likelihood of droplet transmission.

This study is based on epidemiological theory and examines the impacts of vaccination, symptomatic infections and asymptomatic infections. As a result, we formulate an SVPEAIRS model that follows the principles of periodic disease transmission. Firstly, the spectral radius of the linear integral operator is used to define the basic reproduction number $\mathcal{R}_0$, which is crucial for determining whether the disease will be eradicated or continue to spread. The main research findings show that when $\mathcal{R}_0 < 1$, the disease-free equilibrium $\mathcal{M}_0$ of system (2.1) is globally asymptotically stable, indicating that the disease eventually become extinct. Conversely, when $\mathcal{R}_0 > 1$, the disease persists, and there exists a positive ω-periodic solution. Additionally, we conduct numerical simulations of system (2.1), which further validate the main theoretical results of the system (2.1). Figure 2 shows that the fitting curve for rubella closely matches the actual data. Using the least squares method, we estimate the parameter $\beta(t)$ and obtain $\mathcal{R}_0 = 0.9367$ by numerical calculations. These data results indicate that aggressive MMR vaccine and improved recovery rate of infected patients are crucial for preventing rubella infectious diseases. Finally, based on the bifurcation diagrams in Figure 6, we analyze the impact of the transmission rate on both symptomatic and asymptomatic infections.

This study establishes a periodic epidemic model that provides a foundational framework for exploring the complex transmission dynamics of diseases such as rubella. Although the current research has revealed the significant influence of seasonal forcing on disease transmission, nonlinear characteristics such as chaotic phenomena and strange attractors in the system remain to be further explored. Future studies will focus on expanding the theoretical dimensions of the generalized model, particularly analyzing the intrinsic relationship between periodic parametric forcing and global dynamics. Specially emphasis on developing a more comprehensive mathematical framework to demonstrate the existence of strange attractors, by referring to [3], it is possible to derive the relevant chaos theory and clarify its implications for disease control strategies. These research directions not only present important mathematical challenges but may also offer new theoretical tools for predicting and controlling seasonal infectious diseases.

Declarations

Ethics approval and consent to participate. Not applicable.

Consent for publication. Not applicable.

Availability of data and materials. The datasets generated during and/or analysed during

the current study are available from the corresponding author on reasonable request.

Competing interests. The authors declared that they have no conflicts of interest to this work.

References

[1] S. O. Adewale, T. O. Oluyo, L. W. Olaitan and J. K. Oladejo, *Mathematical analysis of rubella disease dynamics: The role of vertical transmission and vaccination*, Transpublika International Research in Exact Sciences, 2024, 3(4), 28–43.

[2] D. Aleanu, H. Mohammadi and S. Rezapour, *A mathematical theoretical study of a particular system of Caputo–Fabrizio fractional differential equations for the Rubella disease model*, Advances in Difference Equations, 2020, 2020, 184. DOI: 10.1186/s13662-020-02614-z.

[3] J. P. S. M. de Carvalho and A. A Rodrigues, *Strange attractors in a dynamical system inspired by a seasonally forced SIR model*, Physica D: Nonlinear Phenomena, 2022, 434, 133268. DOI: 10.1016/j.physd.2022.133268.

[4] J. P. S. M. de Carvalho and A. A Rodrigues, *Pulse vaccination in a SIR model: Global dynamics, bifurcations and seasonality*, Communications in Nonlinear Science and Numerical Simulation, 2024, 139, 108272. DOI: 10.1016/j.cnsns.2024.108272.

[5] P. Van den Driessche and J. Watmough, *Reproduction numbers and sub-threshold endemic equilibria for compartmental models of disease transmission*, Mathematical Biosciences, 2002, 180(1–2), 29–48.

[6] M. Han and Y. Ye, *On the stability of periodic solutions of piecewise smooth periodic differential equations*, Acta Mathematica Scientia, 2024, 44(4), 1524–1535.

[7] A. Hurford, X. Wang and X.-Q. Zhao, *Regional climate affects salmon lice dynamics, stage structure and management*, Proceedings of the Royal Society B, 2019, 286. DOI: 10.1098/rspb.2019.0428.

[8] I. Koca, *Analysis of rubella disease model with non-local and non-singular fractional derivatives*, An International Journal of Optimization and Control: Theories and Applications, 2018, 8(1), 17–25.

[9] Z. Li and T. Zhang, *Analysis of a COVID-19 epidemic model with seasonality*, Bulletin of Mathematical Biology, 2022, 84, 146. DOI: 10.1007/s11538-022-01105-4.

[10] Z. Li and X.-Q. Zhao, *Global dynamics of a nonlocal periodic reaction-diffusion model of Chikungunya disease*, Journal of Dynamics and Differential Equations, 2024, 36(4), 3073–3107.

[11] Y. Ma, K. Liu, W. Hu, S. Song, S. Zhang and Z. Shao, *Epidemiological characteristics, seasonal dynamic patterns, and associations with meteorological factors of Rubella in Shaanxi Province, China, 2005–2018*, The American Journal of Tropical Medicine and Hygiene, 2020, 104, 166–174. DOI: 10.4269/AJTMH.20-0585.

[12] F. O. Ochieng, *SEIRS model for malaria transmission dynamics incorporating seasonality and awareness campaign*, Infectious Disease Modelling, 2024, 9(1), 84–102.

[13] B. P. Prawoto, A. Abadi and R. Artiono, *Dynamic of re-infection rubella transmission model with vaccination*, AIP Conference Proceedings, 2020, 2264(1), 020005.

[14] M. M. Al Qurashi, *Role of fractal-fractional operators in modeling of rubella epidemic with optimized orders*, Open Physics, 2020, 18(1), 1111–1120.

[15] P. Strebel, M, Grabowsky and E. Hoekstra, A. Gay and S. Cochi, *Evolution and contribution of a global partnership against measles and rubella, 2001–2023*, Vaccines, 2024, 12(6), 693. DOI: 10.3390/VACCINES12060693.

[16] G. T. Tilahun, T. M. Tolasa, M. D. Asfaw and G. A. Wole, *Stochastic and deterministic models for rubella dynamics with two doses of vaccination and vertical transmission*, Discrete Dynamics in Nature and Society, 2024. DOI: 10.1155/2024/9697951.

[17] G. T. Tilahun, T. M. Tolasa and G. A. Wole, *Modeling the dynamics of rubella disease with vertical transmission*, Heliyon, 2022, 8(11), e11794. DOI: 10.1016/j.heliyon.2022.e11797.

[18] W. Wang and X.-Q. Zhao, *Threshold dynamics for compartmental epidemic models in periodic environments*, Journal of Dynamics and Differential Equations, 2008, 20(3), 699–717.

[19] World Health Organization, *Immunological basis for immunization: Module 11: Rubella*, 2008. https://www.who.int/publications/i/item/9789241596848.

[20] World Health Organization, *Surveillance guidelines for measles, rubella and congenital rubella syndrome in the WHO European Region*, 2012. https://pesquisa.bvsalud.org/portal/resource/pt/biblio-1053404.

[21] H. M. Yang and A. R. R. Freitas, *Biological view of vaccination described by mathematical modellings: From rubella to dengue vaccines*, Math. Biosci. Eng., 2019, 16(4), 3195–3214.

[22] X.-Q. Zhao, *Dynamical Systems in Population Biology*, Springer International Publishing, New York, 2017.

[23] F. Zhang and X.-Q. Zhao, *A periodic epidemic model in a patchy environment*, Journal of Mathematical Analysis and Applications, 2007, 325(1), 496–516.

Received March 2025; Accepted November 2025; Available online December 2025.